

# Neutron scattering study of soft phonons and diffuse scattering in insulating $\text{La}_{1.95}\text{Sr}_{0.05}\text{CuO}_4$

Shuichi Wakimoto,<sup>1,\*</sup> Seunghun Lee,<sup>2</sup> Peter M. Gehring,<sup>2</sup> Robert J. Birgeneau,<sup>1</sup> and Gen Shirane<sup>3</sup>

<sup>1</sup> *Department of Physics, University of Toronto, Toronto, Ontario, Canada M5S 1A7*

<sup>2</sup> *NIST Center for Neutron Research, National Institute of Standards and Technology, Gaithersburg, Maryland 20889-8562, USA*

<sup>3</sup> *Department of Physics, Brookhaven National Laboratory, Upton, New York 11973-5000, USA*

(Dated: June 27, 2018)

Soft phonons and diffuse scattering in insulating  $\text{La}_{2-x}\text{Sr}_x\text{CuO}_4$  ( $x = 0.05$ ) have been studied by the neutron scattering technique. The X-point phonon softens from high temperature towards the structural transition temperature  $T_s = 410$  K, and the Z-point phonon softens again below 200 K. The Z-point phonon softening persists to low temperature, in contrast to the behavior observed in the superconducting  $x = 0.15$  compound, in which the Z-point phonon hardens below  $T_c$ . The diffuse scattering associated with the structural phase transition at 410 K appears at commensurate positions. These results highlight interesting differences between superconducting and insulating samples.

## I. INTRODUCTION

No direct connection between the unusual superconductivity and the lattice dynamics in the cuprate high- $T_c$  materials has been established to date. By contrast, two of the most successful demonstrations of such a connection in BCS materials were reported for  $\text{Nb}_3\text{Sn}$  (Ref. 1) and for Nb (Ref. 2) by neutron inelastic scattering techniques to show that acoustic phonons with energies less than the superconducting gap energy soften and exhibit linewidths that decrease below  $T_c$ . The smaller linewidths correspond to longer phonon lifetimes, and result from the absence of any decay channel available to such phonons in the presence of the superconducting gap which opens up at  $T_c$ . Although such behaviour has not been confirmed for the high- $T_c$  cuprate  $\text{La}_{2-x}\text{Sr}_x\text{CuO}_4$  (LSCO) system, low-energy soft phonons have been reported to show interesting correlations with the superconductivity. Firstly, an anomalous lattice hardening below  $T_c$  has been observed by ultrasonic measurements<sup>3</sup>. Later, it was found that the soft phonon associated with the tilting mode of the  $\text{CuO}_6$  octahedra hardens, and that the phonon linewidth saturates below  $T_c$ .<sup>4,5</sup>

Another interesting feature has been studied in the high-temperature-tetragonal (HTT) phase of LSCO with  $x = 0.12$ , where Kimura *et al.*<sup>5</sup> have found that the diffuse scattering appears at incommensurate (IC) lattice positions located around the X-points,  $(n/2, n/2, 2l)$ , as shown by the open circles in Fig. 1 (a). Intriguingly, the incommensurability saturates at the same value as that exhibited by the IC static (or dynamic) antiferromagnetic peaks, which suggests that a correlation may exist between the superconductivity, magnetism, and lattice distortion. In this paper, we report the results of neutron scattering experiments performed on a single crystal sample of insulating  $\text{La}_{1.95}\text{Sr}_{0.05}\text{CuO}_4$  that were designed to test if the features of the soft phonons and the diffuse scattering mentioned above are in fact related to the superconductivity. Our results bring to light an interesting contrast between superconducting and insulating sam-

ples of LSCO.

## II. SCATTERING GEOMETRY AND EXPERIMENTAL DETAILS

The high-temperature structure of LSCO is tetragonal (space group  $I4/mmm$ ), and it is known that an instability of the zone boundary X-point soft phonon causes a displacive structural transition to the low-temperature orthorhombic (LTO) phase (space group  $Bmab$ ).<sup>6,7,8</sup> The left side of Fig. 1 depicts the reciprocal lattice of the HTT phase ( $T > T_s$ , where  $T_s$  is structural transition temperature), and the LTO phase ( $T < T_s$ ). Due to the twinned structure of the crystal, the  $[HH0]$  axis in the HTT phase becomes a superposition of the  $[H00]$  and  $[0K0]$  axes in the LTO phase. In the HTT phase, IC diffuse scattering has been observed for a superconducting  $x = 0.12$  sample around the X-points as shown by open circles.<sup>5</sup> In the LTO phase, superlattice peaks appear at reciprocal lattice points such as (014) and (032), shown by the open squares, which become zone-center  $\Gamma$ -points, while positions such as (104) and (302) become zone-boundary Z-points.

Thus the structural transition lifts the degeneracy of the X-point phonon, and two modes can be distinguished in the LTO phase, i.e. the  $\Gamma$ -point and the Z-point phonons, which correspond to the octahedral tilting mode along the orthorhombic  $b$ - and  $a$ -axis, respectively. The  $\Gamma$ - and Z-point phonons harden upon cooling below  $T_s$ , but then the Z-point phonon softens subsequently at lower temperatures, implying an instability against a low-temperature tetragonal ( $P4_2/nm$ ) or low-temperature less-orthorhombic ( $Pccn$ ) phase.<sup>8</sup> In superconducting samples it has been reported that this Z-point softening breaks at  $T_c$ , suggesting that the superconducting state stabilizes the LTO phase.<sup>4,5</sup>

In the present study, Z-point phonons were measured at the (104) and (302) reciprocal lattice points, respectively, using the SPINS and BT9 spectrometers located

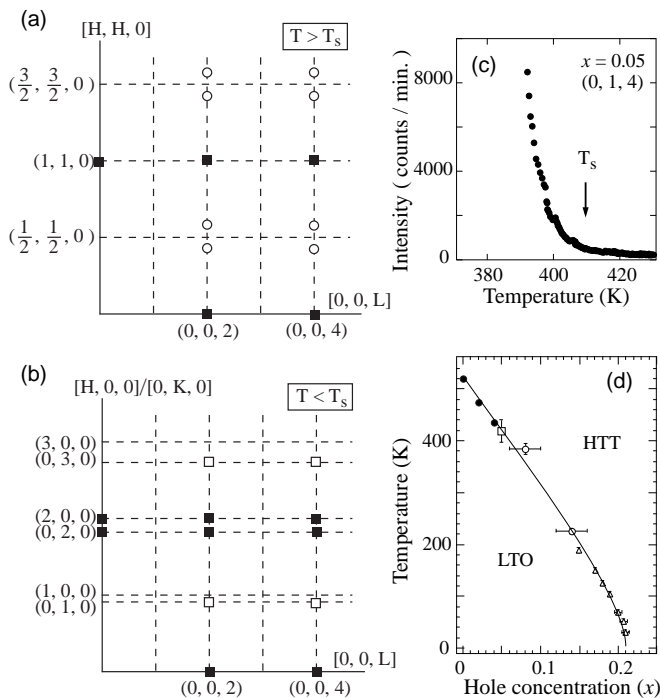


FIG. 1: The reciprocal lattice of LSCO is shown at temperatures (a) above and (b) below the structural transition temperature  $T_s$ . Closed squares represent nuclear Bragg peaks, while open squares represent superlattice peaks in the LTO phase. The open circles correspond to the IC diffuse scattering in the HTT phase observed for  $x = 0.12$  by Kimura *et al.*<sup>5</sup> (c) Temperature dependence of the superlattice peak intensity for  $x = 0.05$ . (d)  $T_s$  as a function of doping  $x$ . The lone open square corresponds to the crystal studied in this paper. The closed circles, open circles, and open triangles represent data taken from Ref. 13, 8, and 14, respectively.

at the NIST Center for Neutron Research. The (104) Z-point phonon was measured using a fixed final neutron energy  $E_f = 5$  meV and horizontal beam collimations 32'-80'-S-80'-open (S = sample), while the (302) Z-point phonon was measured using a fixed initial neutron energy  $E_i = 14.7$  meV and collimations of 40'-22'-S-24'-open. In addition, X-point phonons were studied at  $(1/2, 1/2, 4)$  (tetragonal indexing) using SPINS with the same instrument configuration except with a horizontally-focusing analyzer in place of the flat analyzer. A Be filter placed after the sample, and a PG filter placed before the sample, were used to eliminate higher order ( $\lambda/2$ ,  $\lambda/3$ , ...) neutrons for the  $E_f = 5$  meV and  $E_i = 14.7$  meV measurements, respectively.

The single crystal of  $\text{La}_{1.95}\text{Sr}_{0.05}\text{CuO}_4$  used for the present study was grown in a floating zone furnace,<sup>9,10</sup> and is the same sample that was used for the neutron scattering measurements of the diagonal IC magnetic peaks.<sup>11,12</sup> Lattice constants of the LTO phase at room temperature are  $a_o = 5.38$  Å and  $c_o = 13.24$  Å, which correspond to reciprocal lattice units of  $a_o^* = 1.17$  Å<sup>-1</sup> and  $c_o^* = 0.47$  Å<sup>-1</sup>. The lattice constant in the HTT

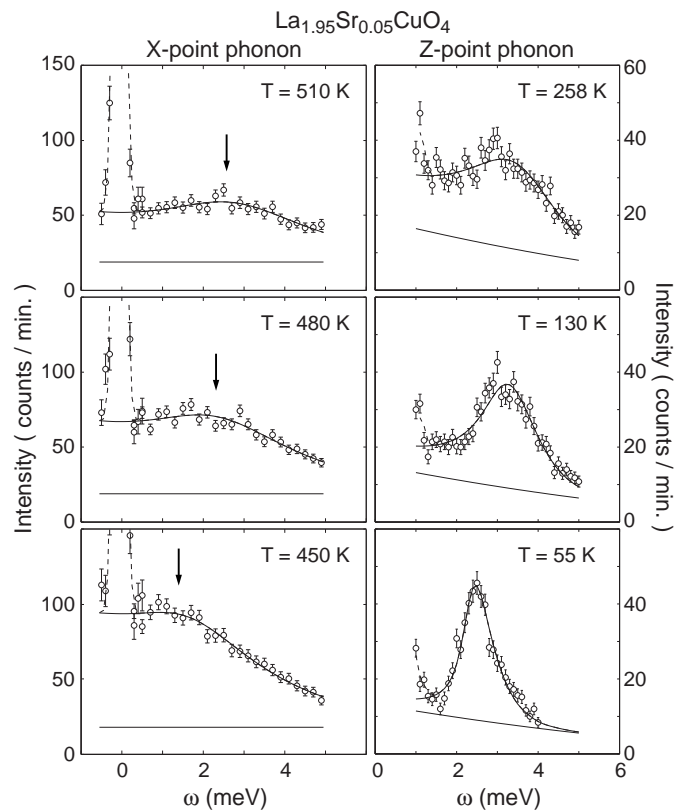


FIG. 2: Left-hand panels show X-point phonons measured at  $\mathbf{Q} = (1/2, 1/2, 4)_{tetra}$  at three temperatures using the SPINS spectrometer with the final neutron energy fixed at 5 meV. Right-hand panels show Z-point phonons measured at  $\mathbf{Q} = (3, 0, 2)_{ortho}$  at three temperatures using the BT9 spectrometer with the initial neutron energy fixed at 14.7 meV. The solid lines are the results of fits to the Lorentzian function specified in the text, convoluted with the instrumental resolution function.

phase is related to that of the LTO phase by  $a_t \sim a_o/\sqrt{2} = 3.80$  Å, thus  $a_t^* \sim 1.65$  Å<sup>-1</sup>. The structural transition temperature  $T_s \sim 410$  K was determined by monitoring the temperature dependence of the superlattice peak intensity at (014), the data for which are shown in Fig. 1 (c). This value is in excellent agreement with the  $x$ -dependence of  $T_s$  accumulated from previous measurements<sup>8,13,14</sup> shown in Fig. 1 (d), where the  $x = 0.05$  data point is represented by an open square.

### III. SOFT PHONON AND DIFFUSE SCATTERING

Representative spectra of the X- and Z-point phonons are shown in Fig. 2. While the X-point phonon for  $T > T_s$  is extremely broad in energy, it is nevertheless apparent that the phonon energy decreases on cooling towards  $T_s$ . Below  $T_s$ , the Z-point phonon is well-defined, and its energy and linewidth decrease with decreasing temperature.

Profiles taken at several temperatures were fit to an instrumental resolution-convoluted  $S(\mathbf{q}, \omega)$  function,

$$S(\mathbf{q}, \omega) = (n(\omega) + 1)I_{ph}L(\mathbf{q}, \omega) + I_G \exp(-\omega^2/2\sigma^2) + I_{BG} \quad (1)$$

$$L(\mathbf{q}, \omega) = \frac{\gamma^2}{(\omega - \omega_{ph})^2 + \gamma^2} + \frac{\gamma^2}{(\omega + \omega_{ph})^2 + \gamma^2}, \quad (2)$$

where  $n(\omega) = (e^{\omega/k_B T} - 1)^{-1}$ ,  $\gamma$  represents the phonon energy half-width at half-maximum. The first term in Eq. (1) represents the phonon cross-section, while the second Gaussian term describes elastic peak at  $\omega = 0$ . From the dispersion relation, the  $q$ -dependent phonon energy  $\omega_{ph}$  is given by

$$\omega_{ph}^2 = \omega_0^2 + a_x q_x^2 + a_y q_y^2 + a_z q_z^2, \quad (3)$$

where  $\omega_0$  is the phonon energy at either the X- or Z-point. The dispersion constants  $a_x = 620$ ,  $a_y = 250$ , and  $a_z = 1130$  meVÅ are taken from Ref. 8. Fits of the data to the above function are shown in Fig. 2. The solid lines reflect the Lorentzian component of the soft phonon as well as the background, while the dashed lines represent the  $\omega = 0$  Gaussians. Note that the background for the Z-point profiles slopes as a result of the analyzer correction factor  $k_f^3 / \tan \theta_A$  ( $k_f$  is final neutron wave vector and  $\theta_A$  is the analyzer angle with respect to the scattered beam), which must be applied to fixed- $E_i$  scans.

The parameters obtained from the fits are summarized in Figs. 3 and 4. The temperature dependence of  $\omega_0$  and  $\gamma$  are shown in Fig. 3 (a) and (b), respectively. A general trend is observed on cooling in which the X-point phonon softens towards  $T_s$ , and the Z-point phonon recovers below  $T_s$  and then softens again below  $\sim 200$  K. Meanwhile, the linewidth  $\gamma$  also starts to decrease with decreasing temperature below  $\sim 200$  K. Around  $T_s$ , the phonon profiles measured at SPINS (not shown) are not well-defined, possibly because they overlap with a  $\Gamma$ -point phonon that may not be high enough in energy to resolve from the Z-point phonon, and in part because of the strongly damped nature of the soft phonons at high temperatures. Thus we were not able to determine if the phonon softens completely at the structural transition temperature.

An enlarged figure of  $\omega_0$  that covers the temperature range  $0 \leq T \leq 100$  K is shown in Fig. 4 (a) together with the data for  $x = 0.15$  reported by Lee *et al.*<sup>4</sup> The  $\omega_0$  of the insulating  $x = 0.05$  sample decreases monotonically with decreasing temperature while the superconducting  $x = 0.15$  compound exhibits a softening that breaks at  $T_c$ . On the other hand, as shown in the enlarged Fig. 4 (b), the linewidth  $\gamma$  for  $x = 0.05$  decreases with temperature and saturates below  $\sim 30$  K, which is similar to the behavior of  $\gamma$  in superconducting samples, which saturates around  $T_c \sim 35$  K (Ref. 4,5). Thus soft phonons show both contrasting and similar behavior in insulating and superconducting samples.

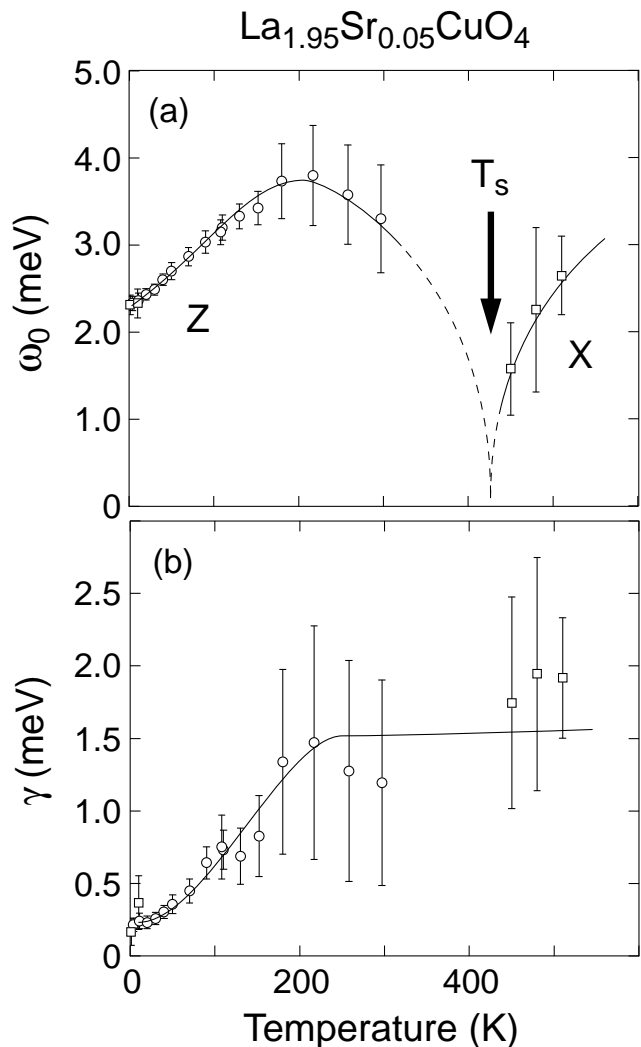


FIG. 3: Temperature dependence of (a) the soft phonon energy  $\omega_0$  and (b) the phonon energy linewidth  $\gamma$ . The lines are guides-to-the-eye. The squares and circles depict the data taken at  $(1, 0, 4)$  (SPINS) and  $(3, 0, 2)$  (BT9), respectively.

Another important contrast between insulating and superconducting materials is found in the diffuse scattering in the HTT phase. As mentioned in Sec. I, Kimura *et al.*<sup>5</sup> have reported IC diffuse scattering located around the X-point in the HTT phase for a superconducting  $x = 0.12$  sample. However, we observe commensurate diffuse scattering for an insulating  $x = 0.05$  sample. Figure 5 shows diffuse scattering peaks along the  $(1/2 + q, 1/2 + q, 4)$  direction for  $x = 0.05$  represented by open symbols. Commensurate diffuse scattering grows with decreasing temperature towards  $T_s$ , below which it is replaced with a sharp resolution-limited superlattice peak shown by the dashed line in the upper figure. The lower figure also shows the IC diffuse peaks reported by Kimura *et al.* for  $x = 0.12$  measured at 390 K along the  $(3/2 + q, 3/2 + q, 2)$  trajectory for comparison. The  $x = 0.05$  data are well-described by fits to a resolution-

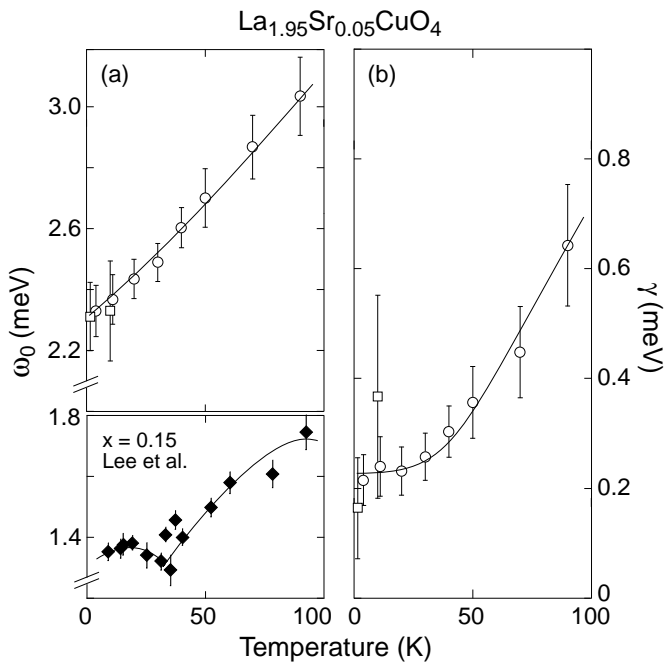


FIG. 4: Enlarged figures of the same data in Fig. 3, covering the range  $0 \leq T \leq 100$  K, are shown. Data for  $x = 0.15$  taken from Ref. 4 are represented by diamonds in (a). Lines are guides to the eye. The squares and circles depict the data taken at  $(1, 0, 4)$  (SPINS) and  $(3, 0, 2)$  (BT9), respectively.

convoluted two-dimensional Lorentzian centered at the commensurate position, as shown by the solid lines with a half-width at half-maximum  $\kappa = 0.07 \text{ \AA}^{-1}$  for 420 K and  $\kappa = 0.09 \text{ \AA}^{-1}$  for 450 K.

#### IV. DISCUSSION

We report soft phonon and diffuse scattering measurements on an insulating  $x = 0.05$  LSCO sample with the goal of elucidating any intrinsic relationship that may exist between the superconductivity and lattice instability exhibited by these materials. A comparison between the data taken on the present insulating sample and previously reported superconducting samples of LSCO reveals some important contrasts.

Firstly, there is no break in the softening of the Z-point phonon in the insulating sample (Fig. 4 (a)). This reveals a robust correlation between superconductivity and the structural instability as discussed previously.<sup>3,4,5</sup> On the other hand, the linewidths of the Z-point phonon for both insulating ( $x = 0.05$ ) and superconducting ( $x = 0.10, 0.12$ , and  $0.15$  (Refs. 4,5)) samples saturate at low temperatures. This suggests that the saturation of the linewidth is not due purely to the superconducting state. A possible alternative explanation is that the saturated value is determined by impurity scattering from the dopant Sr atoms, since the saturated value increases monotonically with  $x$ . The hole concen-

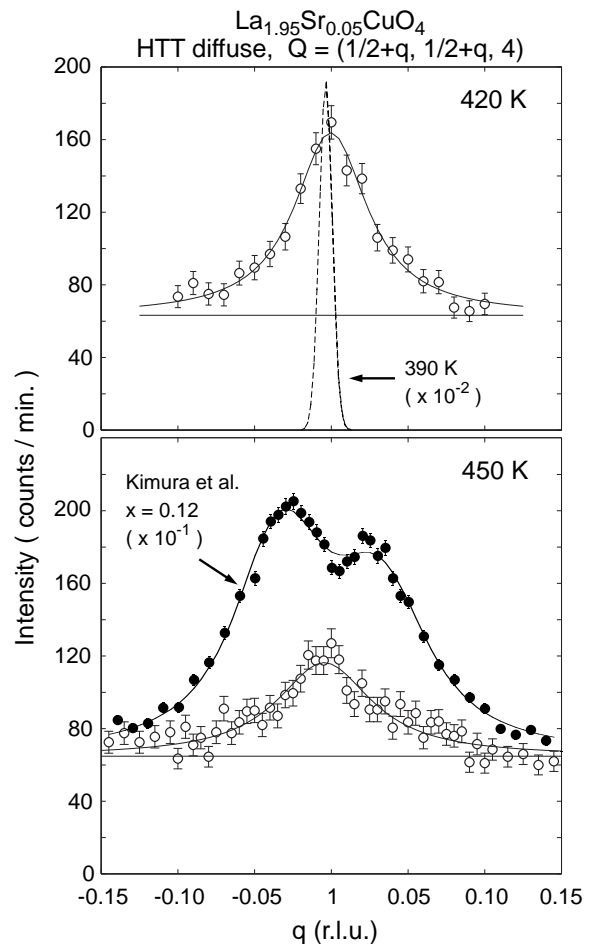


FIG. 5: Diffuse scattering profiles measured along the  $(1/2 + q, 1/2 + q, 4)$  trajectory. The superlattice peak measured at 390 K is also shown as a dashed line in the upper figure. The solid lines are fits to the resolution-convoluted two-dimensional Lorentzian function plus background. The lower figure also shows IC diffuse scattering in the HTT phase of the  $x = 0.12$  sample<sup>5</sup>, which has a  $T_s$  of 240 K.

tration  $x$  and saturated value of  $\gamma_0$  are summarized in Table 1. The dependence of  $\gamma_0$  is roughly linear with  $x$ .

Briefly, it might be also interesting to consider if there is any significance to the maximum value of  $\omega_0$  of the Z-point phonon. Needless to say, the temperature where this maximum value is achieved changes with the transition temperature  $T_s$ . However, for both  $x = 0.05$  and  $0.15$  samples, the Z-point phonon starts to soften at the temperature where the linewidth  $\gamma$  coincidentally starts to decrease, suggesting a general correlation between phonon lifetime and lattice instability.

Secondly, the diffuse scattering in the HTT phase is commensurate in the insulating sample. This suggests that the incommensurate nature of the diffuse scattering is characteristic of the superconducting sample, or characteristic near the specific concentration  $x = 0.12$  where the IC spin density wave order is well established at low temperatures.<sup>15,16</sup> Moreover, the incommensura-

TABLE I: Hole concentration  $x$  and saturated linewidth  $\gamma_0$ . Note that the linewidth in Ref. 4 is defined as  $2\gamma$ .

| $x$  | $\gamma_0$ (meV) | Ref.    |
|------|------------------|---------|
| 0.0  | 0.10             | 4       |
| 0.05 | 0.22             | present |
| 0.10 | 0.38             | 5       |
| 0.12 | 0.55             | 5       |
| 0.15 | 0.38             | 4       |

bility of the diffuse scattering increases with temperature and saturates at the same value as that of the magnetic IC modulation.<sup>17</sup> In either case, the IC diffuse scattering appears at much higher temperatures than those where the charge localization behavior has been observed by the NQR wipeout effect<sup>18</sup> or by conductivity measurements.<sup>19</sup>

Our current experiment on the  $x = 0.05$  sample has established the relation between the incommensurate diffuse peak and the superconductivity. The previous study by Kimura *et al.*<sup>5</sup> on samples with  $0.10 \leq x \leq 0.12$  can

now be interpreted as an explicit signature of an incipient lattice modulation of the hole doped cuprate superconductors that may be related to the inhomogeneous charge and spin state such as the stripes. It would be interesting in future studies to examine diffuse scattering in  $x = 0.07$ , which is just above the superconducting transition, as well as that in optimally doped  $x = 0.15$  and overdoped  $x = 0.20$  samples.

### Acknowledgments

The authors thank M. Fujita, G. Gu, A. Kagedan, H. Kimura, C. Stock, J. M. Tranquada, and S. Ueki for invaluable discussions. The present work was supported by the US-Japan Cooperative Research Program on Neutron Scattering. Work at the University of Toronto is part of CIAR and supported by NSERC of Canada, while research at BNL is supported by the U. S. DOE under contact No. DE-AC02-98CH10886. The work on SPINS is based upon activities supported by the National Science Foundation under Agreement No. DMR-9986442.

\* Corresponding author: waki@physics.utoronto.ca

<sup>1</sup> J. D. Axe and G. Shirane, Phys. Rev. Lett. **30**, 214 (1973).

<sup>2</sup> S. M. Shapiro, G. Shirane, and J. D. Axe, Phys. Rev. B **12**, 4899 (1975).

<sup>3</sup> M. Nohara, T. Suzuki, Y. Maeno, T. Fujita, I. Tanaka, and H. Kojima, Phys. Rev. Lett. **70**, 3447 (1993).

<sup>4</sup> C.-H. Lee, K. Yamada, M. Arai, S. Wakimoto, S. Hosoya, and Y. Endoh, Physica C **257**, 264 (1996).

<sup>5</sup> H. Kimura, K. Hirota, C.-H. Lee, K. Yamada, and G. Shirane, J. Phys. Soc. Jpn. **69**, 851 (2000).

<sup>6</sup> R. J. Birgeneau, C. Y. Chen, D. R. Gabbe, H. P. Jenssen, M. A. Kastner, C. J. Peters, P. J. Picone, T. Thio, T. R. Thurston, and H. L. Tuller, Phys. Rev. Lett. **59**, 1329 (1987).

<sup>7</sup> P. Böni, J. D. Axe, G. Shirane, R. J. Birgeneau, D. R. Gabbe, H. P. Jenssen, M. A. Kastner, C. J. Peters, P. J. Picone, and T. R. Thurston, Phys. Rev. B **38**, 185 (1988).

<sup>8</sup> T. R. Thurston, R. J. Birgeneau, D. R. Gabbe, H. P. Jenssen, M. A. Kastner, P. J. Picone, N. W. Preyer, J. D. Axe, P. Böni, G. Shirane, M. Sato, K. Fukuda, and S. Shamoto, Phys. Rev. B **39**, 4327 (1989).

<sup>9</sup> S. Hosoya, C. H. Lee, S. Wakimoto, K. Yamada, and Y. Endoh, Physica C **235-240**, 547 (1994).

<sup>10</sup> C. H. Lee, N. Kaneko, S. Hosoya, K. Kurahashi, S. Wakimoto, K. Yamada, and Y. Endoh, Semicond. Sci. Technol. **11**, 981 (1998).

<sup>11</sup> S. Wakimoto, G. Shirane, Y. Endoh, K. Hirota, S. Ueki, K. Yamada, R.J. Birgeneau, M.A. Kastner, Y.S. Lee, P.M.

Gehring and S.H. Lee, Phys. Rev. B **60**, R769 (1999).

<sup>12</sup> S. Wakimoto, R. J. Birgeneau, M. A. Kastner, Y. S. Lee, R. Erwin, P. M. Gehring, S. H. Lee, M. Fujita, K. Yamada, Y. Endoh, K. Hirota, and G. Shirane, Phys. Rev. B **61**, 3699 (2000).

<sup>13</sup> B. Keimer, N. Belk, R. J. Birgeneau, A. Cassanho, C. Y. Chen, M. Greven, M. A. Kastner, A. Aharony, Y. Endoh, R. W. Erwin, and G. Shirane, Phys. Rev. B **46**, 14034 (1992).

<sup>14</sup> H. Takagi, R. J. Cava, M. Marezio, B. Batlogg, J. J. Krajewski, W. F. Peck, Jr., P. Bordet, and D. E. Cox, Phys. Rev. Lett. **68**, 3777 (1992).

<sup>15</sup> T. Suzuki, T. Goto, K. Chiba, T. Shinoda, T. Fukase, H. Kimura, K. Yamada, M. Ohashi, and Y. Yamaguchi, Phys. Rev. B **57**, 3229 (1998).

<sup>16</sup> H. Kimura, K. Hirota, H. Matsushita, K. Yamada, Y. Endoh, S. -H. Lee, C. F. Majkrzak, R. Erwin, G. Shirane, M. Greven, Y. S. Lee, M. A. Kastner, and R. J. Birgeneau, Phys. Rev. B **59**, 6517 (1999).

<sup>17</sup> K. Yamada, C. H. Lee, K. Kurahashi, S. Wakimoto, S. Ueki, H. Kimura, Y. Endoh, S. Hosoya, G. Shirane, R. J. Birgeneau, M. Greven, M. A. Kastner, and Y. J. Kim, Phys. Rev. B **57**, 6165 (1998).

<sup>18</sup> A. W. Hunt, P. M. Singer, K. R. Thurber, and T. Imai, Phys. Rev. Lett. **82**, 4300 (1999).

<sup>19</sup> S. Komiya and Y. Ando, Phys. Rev. B **70**, 060503 (2004).